# Nonlinear Optical Properties and Chromophore Electrostatic Interactions for the Poly(ether ketone) Guest−Host Polymer Films

**Shi Wei,*,† Zhang Zhenyu,‡ Pan Qiwei,† Gu Qingtian,† Ye Lina,§ Fang Changshui,† Xu Dong,† Wei Hongzhen,⊥ and Yu Jinzhong⊥**

*State Key Laboratory of Crystal Materials, Shandong University, Jinan 250100, P. R. China; Department of Chemistry, Shandong University, Jinan 250100, P. R. China; Institute of Optoelectronics, Department of Physics, Shandong University, Jinan 250100, P. R. China; and Semiconductor Institute Region of State Key Laboratory on Integrated Optoelectronics, Chinese Academy of Science, Beijing 100083, P. R. China*

*Received October 6, 2000; Revised Manuscript Received January 10, 2001*

ABSTRACT: The poly(ether ketone) (PEK-c) guest−host system thin films doped with different weight percents of 3-(1,1-dicyanothenyl)-1-phenyl-4,5-dihydro-1*H*-pryazole (DCNP) were prepared. Their second-order nonlinear optical (NLO) coefficients $\chi_{33}^{(2)}$ were measured by using the Maker fringe method through in-situ second-harmonic-generation (SHG) probing. Experimental results indicated that, at high chromophore loading in the polymer system, the second-order NLO properties of the poled polymer films could decrease with increasing chromophore loading. In this paper, the relationship between the macroscopic second-order NLO coefficient and the chromophore number density was investigated by considering the role of the electrostatic interactions of chromophores in the polymer films. According to the improved relationship, the macroscopic second-order NLO coefficient is no longer in a direct ratio with the chromophore number density in the polymer films, especially when the chromophore loading is high. The effect of the electrostatic interactions of chromophores on second-order NLO properties was discussed from the improved relationship.

## Introduction

The development of thin film polymer materials that are suitable for the fabrication of high-speed integrated optical devices is presently a major focus of research in nonlinear optics.[1−3] Polymer materials have been demonstrated to possess large nonlinear optical (NLO) activity compared to traditional inorganic materials, and the intrinsic low dielectric constant, ease of processing into films, and compatibility with microelectronic processes are the other major advantage of the polymers. Especially due to the research and development of the wavelength-division multiplexing (WDM) all-optical communication network, the ultrafast response characteristics of the NLO polymers are more outstanding.[1,3] Polymer materials have been regarded as the key materials of the devices (such as polymer waveguide modulators and switches) in the development of the WDM all-optical communication network. Thus, the investigation of the NLO polymer from the molecular design to the preparation of the NLO polymer has been developed very fast. At present, the investigations of the poled polymers mainly focus on (a) the improvement of the macroscopic second-order NLO coefficient,[4−6] (b) the high temporal and temperature stability of the NLO properties of the poled polymers,[3,7−9] and (c) low transmission loss.[10,11] To realize large macroscopic NLO properties, Singer's relationship between molecular and macroscopic properties has been directed toward the synthesis of the chromophores with a large product of the ground-state dipole moment $\mu$ and the first hyperpolarizability $\beta$, high number densities of the chromophores in the host polymer, and more efficient poling.[12] To optimize the product $\mu\beta$, two key strategies have been proposed in the design of chromophore molecules.[3] First, the chromophore molecules should have a bridge that loses aromaticity upon polarization but also have an acceptor that gains aromaticity upon polarization. Second, the benzene rings in the chromophore molecules can be replaced with heterocyclic rings, such as thiazole and thiophene. Among the NLO polymer systems where chromophores are incorporated in the polymer hosts, the guest−host polymer system does not require chemical attachment of a chromophore to a host polymer. It can be fabricated at a lower cost than any other system, such as side-chain, cross-linked, and main-chain polymers, all of which are synthesized with more complicated reactions. And the guest−host polymer system always has more efficient poling than side-chain, cross-linked, and main-chain systems. However, in general, the guest−host system has two disadvantages: the decay of the NLO properties is fast, and the chromophore concentration in the polymer system is low. Recently, we demonstrated the approach to overcome these disadvantages by using a high-$T_g$ (glass transition temperature) host polymer poly(ether ketone) (PEK-c) doped with organic chromophore 3-(1,1-dicyanothenyl)-1-phenyl-4,5-dihydro-1*H*-pryazole (DCNP) that has good miscibility with the host polymer. Guest−host thin films in which the range of the weight percent of DCNP is from 20% to 50% were prepared. Their second-order NLO properties were investigated by using in-situ second-harmonic-generation (SHG) signal measurement. A large second-order NLO coefficient $\chi_{33}^{(2)} = 142.5 \times 10^{-12}$ m/V was obtained when the doped percent of DCNP is 40 wt % in the DCNP/PEK-c polymer system.

† State Key Laboratory of Crystal Materials, Shandong University.
‡ Department of Chemistry, Shandong University.
§ Department of Physics, Shandong University.
⊥ Chinese Academy of Science.
* Corresponding author: E-mail csfang@icm.sdu.edu.cn; phone 0531-8564451-8012; Fax 0531-8565403.

10.1021/ma001737b CCC: $20.00 
Published on Web 02/16/2001

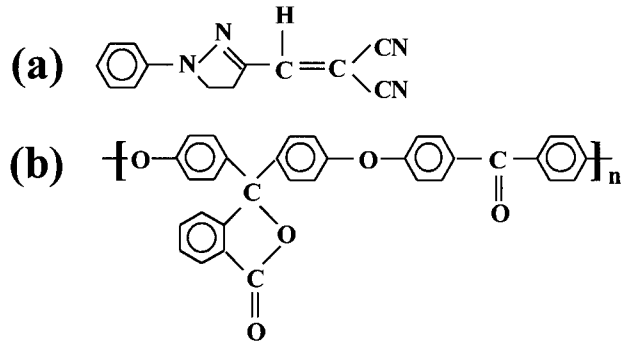


**Figure 1.** (a) Molecular structure of DCNP chromophore and (b) general structure of PEK-c polymer host.

However, when the doped percent of DCNP is above 40 wt %, the second-order NLO coefficient decreases with the doped concentration increasing. In this paper, the attenuation of the macroscopic optical nonlinearities at high chromophore loading is discussed. Because the chromophores always have large polarity, the effect of the chromophore electrostatic interactions on their electric-induced orientational order should be considered when the chromophore loading is high in the polymer system.[13,14] This attenuation of the macroscopic optical nonlinearities can be demonstrated by the role of chromophore electrostatic interactions at high chromophore loading in the guest−host polymer systems.

## Experiments and Results

Chromophore DCNP is a highly conjugated molecule based on substituted dihydropyrazole. The molecular structure of this molecule is shown in Figure 1a, its molecular ground-state dipole moment $\mu$ is 7.0 D,[15] and its hyperpolarizability is $\beta = 44.7 \times 10^{-30}$ esu at zero energy. The host polymer PEK-c is a highly transparent polymer with high glass transition temperature $T_g \sim$ 228 °C. Its general structure is shown in Figure 1b. PEK-c is an ideal polymer host for device fabrication because it is mechanically strong, easily processed into low optical loss thin films, and thermally stable up to 400−500 °C. DCNP and PEK-c were separately dissolved in 1,2-dichloroethane. When guest DCNP and host PEK-c were wholly dissolved in 1,2-dichloroethane, the two solutions were mixed together. Then the premixed solutions were filtered through a syringe with a 0.45 $\mu$m filter attached in order to remove the undissolved impurities. The final polymer solutions can be easily spin-coated onto the indium−tin oxide (ITO) glass substrates to form thin films. Seven kinds of thin films with doped concentrations of DCNP by solid weight percents of 20%, 25%, 30%, 35%, 40%, 45%, and 50% were prepared. After curing at 80 °C for several hours, then by using UV−vis spectrometry, we monitored the films to determine the status of the residual solvent removed. The plasticization introduced by the DCNP guest was determined by DSC (differential scanning calorimeter) measurement (PE DSC-2c). The measured glass transition temperatures of the above seven guest−host systems were 180, 176, 171, 160, 122, 115, and 108 °C, respectively. It was found that the plasticization of the PEK-c host with increasing dopant levels was apparent. The polymer films were poled by the corona-onset poling at elevated temperature (COPET) method. The poling setup as schematically shown in Figure 2 was used. A voltage of +6 kV was applied to the needle electrode. A grid with a bias voltage of +700 V was used

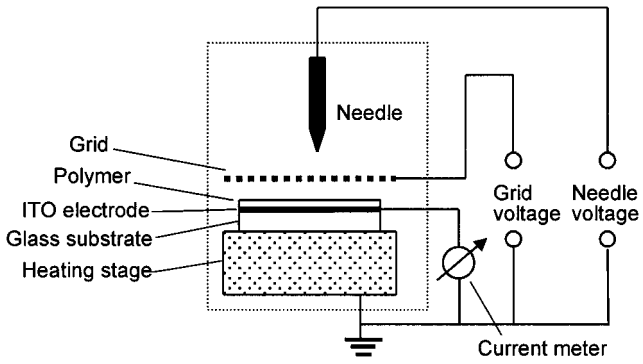


**Figure 2.** Setup for corona poling of polymer films. The samples are mounted on a heating stage, and the current through the polymer sample is determined by an ammeter.

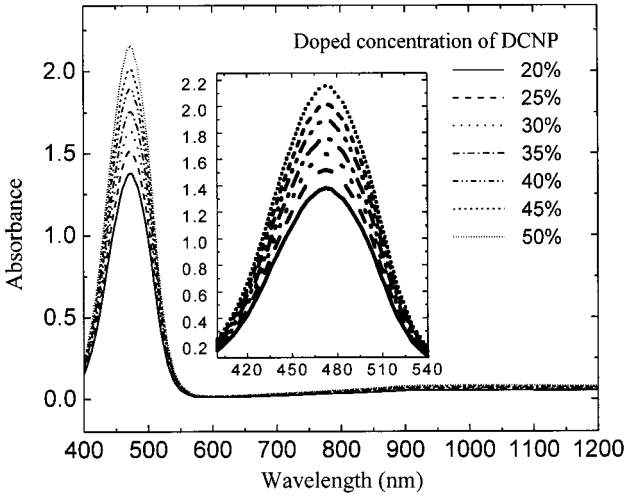


**Figure 3.** Absorption spectra of the poled polymer films with different guest DCNP loading.

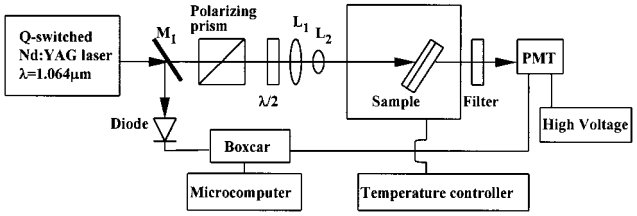


**Figure 4.** Schematic drawing of the experimental setup for in situ signal intensity measurement.

for making the surface-charge distribution uniform. For different polymer films, the poling processes were respectively carried out at just below their $T_g$. They were then cooled to room temperature while maintaining the needle voltage and grid voltage unchanged. The absorption spectra (shown in Figure 3) of the above poled polymer films were measured by using a HITACHI 340 recording spectrophotometer. The second-order NLO coefficient $\chi_{33}^{(2)}$ of the poled polymer films was measured with the Maker fringe method by using the experimental setup shown in Figure 4. The polarized beam of a Q-switched Nd:YAG laser ($\lambda = 1.064$ $\mu$m) at a 10 Hz repetition rate, 150−200 mJ per 10 ns pulse, was focused on the sample with incident angle $\theta$. The fundamental wave was linearly polarized parallel to the plane of incidence and blocked by high-pass filters and a 532 nm interference filter. The SHG signal was detected by a photomultiplier tube (PMT) and then amplified and averaged in a boxcar integrator. The boxcar output was registered by a microcomputer. By

monitoring the SHG signal intensity with respect to the angle of incidence of the fundamental beam, one can determine the second-order NLO coefficients by using the Maker fringe method.[16] If the NLO material has zero absorption for either the fundamental or the SHG wave, the second-order NLO coefficients can be determined by the formulation presented by Jerphagnon and Kurtz.[17] The investigated poled polymer films are absorbing at the SHG wavelength 532 nm (see Figure 3). So we should consider the effect of the absorption in determination of the second-order NLO coefficients using the Maker fringe technique.[18,19] By taking the absorption into effect, Herman and Hayden presented a new formulation of the transmitted SHG power.[19] When the fundamental beam is linearly polarized parallel to the plane of incidence and monitoring only the component of the second-harmonic signal that is similarly polarized, the transmitted SHG power can be written as (neglecting birefringence)[19]

$$P_{2\omega}^{(\gamma\rightarrow \mathrm{p})} = \frac{128\pi^3}{cA}\frac{[t_{\mathrm{af}}^{(1\gamma)}]^4[t_{\mathrm{fs}}^{(2\mathrm{p})}]^2[t_{\mathrm{sa}}^{(2\mathrm{p})}]^2}{n_{2\omega}^2 - \sin^2\theta} P_\omega^2(\chi^{(2)})^2 P^2(\theta) \times \left(\frac{2\pi L}{\lambda}\right)^2 \exp[-2(\delta_\omega + \delta_{2\omega})]\frac{\sin^2\psi + \sinh^2\chi}{\psi^2 + \chi^2} \quad (1)$$

where $\omega$ and $2\omega$ correspond to the fundamental and second-harmonic frequencies, respectively; $P_\omega$ and $P_{2\omega}$ are the optical powers of the fundamental and SHG signals, respectively; $A$ is the cross-sectional area of the fundamental beam; $\chi^{(2)}$ is the appropriate second-order NLO coefficient; $L$ is the thickness of the sample; $\lambda = 1.064\ \mu$m; and $t_{\mathrm{af}}^{(1\gamma)}$, $t_{\mathrm{fs}}^{(2\mathrm{p})}$, and $t_{\mathrm{sa}}^{(2\mathrm{p})}$ are Fresnel transmission coefficients

$$t_{\mathrm{af}}^{(1\gamma)} = \frac{2\cos\theta}{\cos\theta_\omega + n_\omega\cos\theta} \quad (2)$$

$$t_{\mathrm{fs}}^{(2\mathrm{p})} = \frac{2\sqrt{n_{2\omega}^2 - \sin^2\theta}}{(n_{2\mathrm{s}}/n_{2\omega})\sqrt{n_{2\omega}^2 - \sin^2\theta} + (n_{2\omega}/n_{2\mathrm{s}})\sqrt{n_{2\mathrm{s}}^2 - \sin^2\theta}} \quad (3)$$

$$t_{\mathrm{sa}}^{(2\mathrm{p})} = \frac{2\sqrt{n_{2\mathrm{s}}^2 - \sin^2\theta}}{n_{2\mathrm{s}}\cos\theta + (1/n_{2\mathrm{s}})\sqrt{n_{2\mathrm{s}}^2 - \sin^2\theta}} \quad (4)$$

where $n_\omega$ and $n_{2\omega}$ are the refractive indices of the polymer material at frequencies $\omega$ and $2\omega$, respectively, $\theta_\omega$ and $\theta_{2\omega}$ are the angles that the refracted beams make with the normal of the sample surface in the sample at frequencies $\omega$ and $2\omega$, respectively, $n_{2\mathrm{s}}$ is the refractive index of the substrate at frequency $2\omega$, and quantities $P(\theta)$, $\chi$, and $\psi$ are defined below.

Considering the relationship $\chi_{33}^{(2)} = 3\chi_{31}^{(2)}$ for the investigated polymer materials, the projection factor $P(\theta)$ can be given as

$$P(\theta) = \left(\frac{\cos^2\theta_\omega}{3} + \sin^2\theta\right)\sin\theta_{2\omega} + \frac{2}{3}\cos\theta_\omega\sin\theta_\omega\cos\theta_{2\omega} \quad (5)$$

$\delta_\omega$, $\delta_{2\omega}$, and $\chi$ can be expressed as (see Appendix of ref 19)

$$\delta_\omega = \frac{2\pi L}{\lambda}\frac{n_\omega^2\kappa_\omega}{\sqrt{n_\omega^2 - \sin^2\theta}} \quad (6a)$$

$$\delta_{2\omega} = \frac{2\pi L}{\lambda}\frac{n_\omega^2\kappa_\omega}{\sqrt{n_\omega^2 - \sin^2\theta}} \quad (6b)$$

$$\chi = \delta_\omega - \delta_{2\omega} \quad (7)$$

where $\kappa_\omega$ and $\kappa_{2\omega}$ are the extinction coefficients of the polymer thin films at frequency $\omega$ and $2\omega$, respectively. And $\psi$ can be expressed as

$$\psi = \frac{\pi L}{2}\frac{4}{\lambda}(n_\omega\cos\theta_\omega - n_{2\omega}\cos\theta_{2\omega}) \quad (8)$$

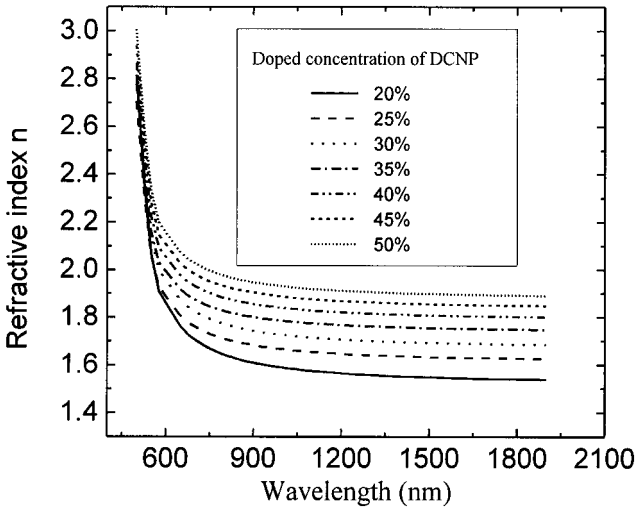


**Figure 5.** Refractive indices of the polymer films for different guest DCNP loading.

The thin films were scanned over a range of $\theta = \pm 60°$ with respect to the direction of the fundamental beam. The refractive index and thickness of each polymer film were measured by using the prism-coupler waveguide method.[20] The thickness of all the polymer film samples is controlled to about 1 $\mu$m by adjusting the concentration of the polymer solutions in solvent and the spin-coating speed and time. The refractive indices of the polymer films for different guest DCNP loading are shown in Figure 5. The dispersion of the refractive index in Figure 5 was obtained by fitting the measured indices (by using the prism-coupler waveguide method) to the Sellmeyer equation. Then the NLO coefficient $\chi_{33}^{(2)}$ of each polymer film can be calculated by using eqs 1−8 and calibrating the experiment with a $Y$-cut quartz reference sample. The measured results of the NLO coefficient $\chi_{33}^{(2)}$ for the investigated polymer films are shown in Figure 6, where $N$ is the number density of the chromophore DCNP in the polymer film and can be related to the weight percent $\Phi$ of DCNP by[21]

$$N = \frac{\Phi N_{\mathrm{A}}\rho_{\mathrm{c}}\rho_{\mathrm{p}}}{M_{\mathrm{w}}[\rho_{\mathrm{c}} - \Phi(\rho_{\mathrm{c}} - \rho_{\mathrm{p}})]} \quad (9)$$

where $N_{\mathrm{A}}$ is Avogadro's number, $M_{\mathrm{w}}$ is the molecular weight of the chromophore DCNP, and $\rho_{\mathrm{c}}$ and $\rho_{\mathrm{p}}$ are the densities of the guest chromophore DCNP and host

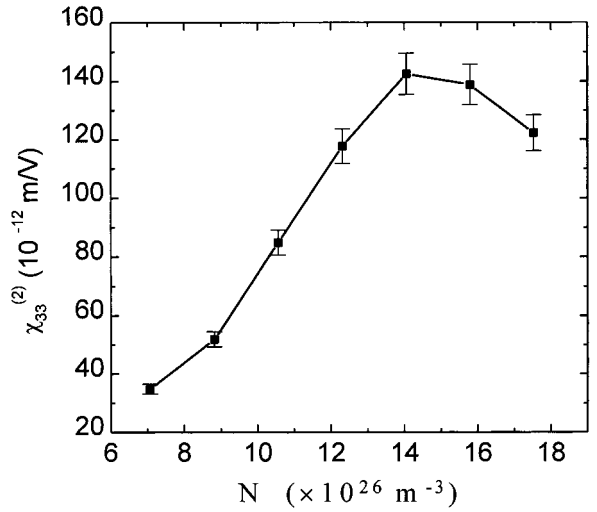


**Figure 6.** Graph of the experimental results in which the second-order NLO coefficients are plotted as a function of the concentrations of the chromophore DCNP for the polymer films.

polymer PEK-c, respectively. From Figure 6, it can be seen that when the number density $N$ is smaller than $14.1 \times 10^{26}$ m$^{-3}$ (or $\Phi < 40\%$), the second-order NLO coefficient $\chi_{33}^{(2)}$ increases nearly linearly with increasing chromophore loading in the polymer film; when $N$ is beyond $14.1 \times 10^{26}$ m$^{-3}$ (or $\Phi > 40\%$), $\chi_{33}^{(2)}$ decreases with increasing $N$; and when $N = 14.1 \times 10^{26}$ m$^{-3}$ (or $\Phi = 40\%$), $\chi_{33}^{(2)}$ has the maximum value $142.5 \times 10^{-12}$ m/V. Thus, it was found that the second-order NLO properties of the poled polymer films could be attenuated when the chromophore loading is high in the polymer system. This kind of attenuation of the macroscopic second-order NLO properties due to the high chromophore loading in the polymer system was also reported by several research groups through their experimental results.[22,23]

## Discussion

To explain the attenuation of the NLO properties of the poled polymer films at high chromophore loading, we calculated the macroscopic second-order NLO coefficients of the DCNP/PEK-c polymer films by considering the chromophore electrostatic interactions using the two-level model.[12] For simple reasons, we ignore the aggregations of chromophores in the following calculations. However, it is obvious that chromophore aggregation mainly results from the chromophore electrostatic interactions, and chromophore aggregation can result in more serious attenuation of the macroscopic second-order NLO properties of the poled polymer films.

For the chromophore DCNP (see Figure 1a), it can be assumed that only one component of the molecular hyperpolarizability, $\beta_{zzz}$, needs to be considered and simply expressed as $\beta$, where the $z$-direction is along the direction of the molecule's permanent dipole moment. The macroscopic second-order NLO coefficient $\chi_{33}^{(2)}$ can be expressed as[12]

$$\chi_{33}^{(2)}(-2\omega;\omega,\omega) = Nf(2\omega)\, f^{2}(\omega)\beta\int\cos^{3}\theta G(\Omega)\,\mathrm{d}\Omega = Nf(2\omega)\, f^{2}(\omega)\beta\langle\cos^{3}\theta\rangle \quad (10)$$

where $\theta$ is the polar angle between the molecular $z$-axis and macroscopic 3-axis (the direction of the poling electric field); the quantity $G(\Omega)$ is a normalized distribution function for the chromophore over the solid angle $\Omega$

$$G(\Omega) = \exp(-U/KT)/\int\mathrm{d}\Omega\,\exp(-U/KT) \quad (11)$$

where $U$ is the energy of the chromophore molecule in the polymer environment, and in an external electric field, the local-field factors are, at optical frequencies

$$f(\omega) = (1/3)(n_{\omega}^{2} + 2); \quad f(2\omega) = (1/3)(n_{2\omega}^{2} + 2) \quad (12)$$

and at low frequency

$$f(0) = \epsilon(n_{\infty}^{2} + 2)/(n_{\infty}^{2} + 2\epsilon) \quad (13)$$

where $n_{\omega}$, $n_{2\omega}$, and $n_{\infty}$ are refractive indices at optical and low frequencies, and $\epsilon$ is the low-frequency dielectric constant.

In the mean-field approximation, the energy $U$ can be given as $U = U_1 + U_2 + U_3$. $U_1$ refers to the interaction between the local poling field and the chromophore permanent dipole moment

$$U_1 = -\mu f(0)E_{\mathrm{p}}\cos\theta \quad (14)$$

$U_2$ refers to the interaction between the local field and the chromophore-induced dipole moment. If we suppose that the polarizability values of the chromophore along the long and short axes are $\alpha_1$ and $\alpha_2$, respectively, and the anisotropy of the polarizability is expressed as $\Delta\alpha = \alpha_1 - \alpha_2$, $U_2$ can be written as[24,25]

$$U_2 = -(1/2)(\alpha_2 + \Delta\alpha\cos^{2}\theta)f^{2}(0)E_{\mathrm{p}}^{2} \quad (15)$$

$U_3$ refers to the chromophore electrostatic interaction[20]

$$U_3 = -(2/R^{6})[(\mu^{4}/KT) + \alpha\mu^{2} + (3/8)\alpha^{2}I] \quad (16)$$

where $R$ is the average chromophore separation in the polymer system, $I$ is the ionization energy of the chromophore molecule, and $\alpha$ is the polarizability of the chromophore molecule. (Here it is regarded that the molecular polarizability is isotropic, and $\alpha = \alpha_1 = \alpha_2$.) In eq 16, the chromophore electrostatic interaction $U_3$ includes the dipole−dipole interaction, the dipole−induced dipole interaction, and the induced dipole−induced dipole interaction.

When ignoring $U_2$ and $U_3$, and supposing $u = \mu f(0)E_{\mathrm{p}}/KT$, we can express $\langle\cos^{3}\theta\rangle$ as a *Langevin* function[12]

$$\langle\cos^{3}\theta\rangle = L_3(u) = [\int\cos^{3}\theta\,\exp(u\cos\theta)\,\mathrm{d}\theta]/[\int\exp(u\cos\theta)\,\mathrm{d}\theta] \quad (17)$$

$L_3(u)$ can be expanded in a power series

$$L_3(u) = \langle\cos^{3}\theta\rangle = L_1(u)[1 - (6/u^{2})] = (u/5) - (u^{3}/105)\cdots \quad (18)$$

When $u \le 1$, eq 18 yields $L_3(u) \approx (u/5)$. Substitution of $L_3(u)$ into eq 10 then yields

$$\chi_{33}^{(2)}(-2\omega;\omega,\omega) = [Nf(2\omega)\, f^{2}(\omega)\, f(0)\mu\beta E_{\mathrm{p}}]/(5KT) \quad (19)$$

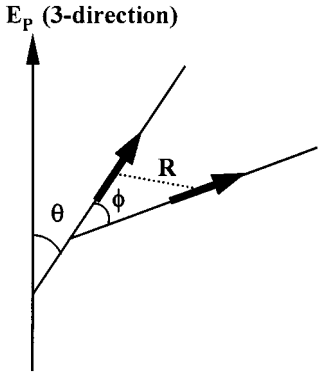


**Figure 7.** Under the approximations of London, the coordinate system defined by an electric poling field and two interacting chromophores. The angle $\theta$ relates a chromophore to the electric poling field, and the angle $\phi$ relates the two interacting chromophores.

or

$$\chi_{33}^{(2)}(-2\omega;\omega,\omega) = [\Phi\rho N_A f(2\omega)\, f^2(\omega)\, f(0)\, E_P(\mu\beta/M_W)]/(5KT) \quad (20)$$

where $\rho$ is the density of the guest−host polymer system. Equations 19 and 20 suggest that the macroscopic second-order NLO coefficient should increase linearly with chromophore weight fraction.

When just ignoring $U_3$, we have $U = U_1 + U_2$, and $\langle\cos^3\theta\rangle$ can be written as[24]

$$\langle\cos^3\theta\rangle = (u/5) - (1/105)\{(u/5)^3 + 8(u/5)[\Delta\alpha f^2(0)E_P{}^2/(2KT)]\} \cdots \quad (21)$$

By comparing eqs 18 and 21, we can find that $U_2$ only leads to an insignificant modification $8(u/5)[\Delta\alpha f^2(0)E_P{}^2/(2KT)]$. Hence, the $U_2$ term of $U$ can be ignored in the following calculation.

In arriving at a description of poling of interacting chromophores, two types of orientational averaging must be considered. One is the averaging over the Euler rotation matrix connecting the chromophore axis system to the laboratory axis system defined by the electric field; another is the averaging over the Euler rotation matrix that relates the interacting chromophores. But with the approximations of London theory, these two types of averaging can reduce to averaging over two single angles $\theta$ and $\phi$, respectively (see Figure 7). Thus, the potential energy $U$ can be written as[26]

$$U = -\mu f(0)E_P \cos\theta - U_3 \cos\phi \quad (22)$$

Carrying out the averaging over $\theta$ and $\phi$ leads to the following poling-induced order parameter relevant to measurement of the macroscopic second-order NLO coefficient[14,27,28]

$$\langle\cos^3\theta\rangle = [\mu f(0)E_P/(5KT)][1 - L^2(U_3/KT)] \quad (23)$$

where $L(U_3/KT) = \coth(U_3/KT) - (KT/U_3)$ is the *Langevin* function. The second term in brackets $[1 - L^2(U_3/KT)]$ represents the attenuation of the order parameter associated with chromophore−chromophore electrostatic interactions. Substitution of eq 23 into eq 10 yields

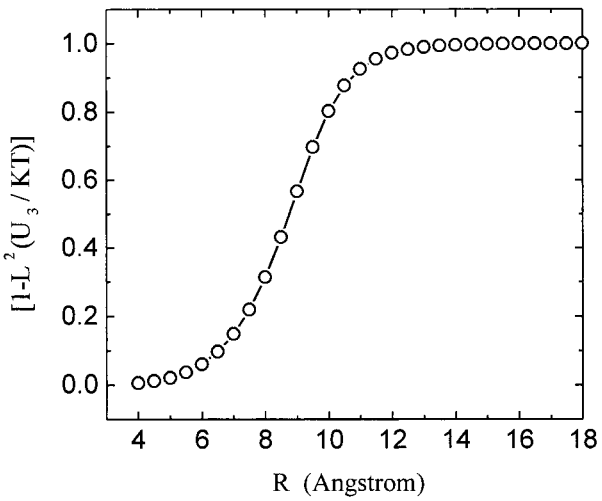


**Figure 8.** Theoretical plot of $[1 - L^2(U_3/KT)]$ vs the average chromophore separation for the DCNP/PEK-c polymer system.

$$\chi_{33}^{(2)}(-2\omega;\omega,\omega) = \{[Nf(2\omega)\, f^2(\omega)\, f(0)\mu\beta E_P]/(5KT)\}[1 - L^2(U_3/KT)] \quad (24)$$

Equation 24 is the relationship that translates microscopic optical nonlinearity into macroscopic optical nonlinearity under considering the chromophore electrostatic interactions. The factor $[1 - L^2(U_3/KT)]$ represents the attenuation of the macroscopic second-order NLO properties associated with the chromophore electrostatic interactions.

For the chromophore DCNP, the molecular permanent dipole moment is 7.0 D.[15] By using the quantum chemistry method AM1, the calculated values of the polarizability and the ionization potential are $\alpha = 5.1 \times 10^{-23}$ cm$^3$ and $I = 7.9 \times 10^{-19}$ J. By using eq 16 and the *Langevin* function $L(U_3/KT)$, we can draw the theoretical plot of $[1 - L^2(U_3/KT)]$ vs the average chromophore separation (Figure 8). As shown in Figure 8, the attenuation factor $[1 - L^2(U_3/KT)]$ decreases dramatically when the chromophore average separation decreases (or, equivalently, the chromophore number density increases) below $R = 10$ Å.

In Figure 9, we show the theoretical plot of the normalized second-order NLO coefficient vs chromophore number density by using eqs 16 and 24. When $N < 11.0 \times 10^{26}$ m$^{-3}$, the NLO properties of the poled polymer film increase linearly with the increasing of DCNP number density $N$. When $N > 11.0 \times 10^{26}$ m$^{-3}$, the NLO properties decrease with increasing $N$ due to the chromophore electrostatic interactions. These lead to a maximum in the graph of the second-order NLO coefficient vs chromophore number density when $N = 11.0 \times 10^{26}$ m$^{-3}$. The above theoretical result agrees well with the experimental result measured by the in-situ SHG signal probing for the DCNP/PEK-c polymer system.

## Conclusions

The NLO polymer DCNP/PEK-c films with doped concentrations of DCNP in percent solid by weight of 20%, 25%, 30%, 40%, 45%, and 50% were prepared. Their macroscopic second-order NLO coefficients

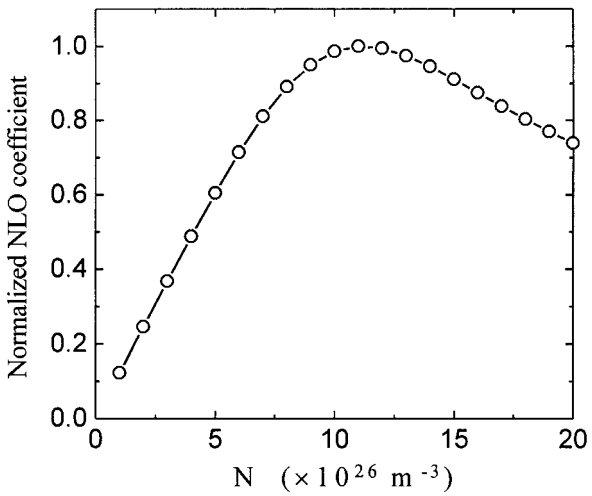


**Figure 9.** Theoretical plot of the normalized second-order NLO coefficient vs chromophore number density for the DCNP/PEK-c polymer system.

were measured by the Maker fringe method. Experimental results indicate that when $N < 14.1 \times 10^{26}$ m$^{-3}$, the macroscopic second-order NLO coefficient $\chi_{33}^{(2)}$ increases nearly linearly with increasing DCNP loading in the DCNP/PEK-c polymer system, when $N < 14.1 \times 10^{26}$ m$^{-3}$, $\chi_{33}^{(2)}$ decreases with increasing $N$, and when $N = 14.1 \times 10^{26}$ m$^{-3}$, $\chi_{33}^{(2)}$ has the maximum value $142.5 \times 10^{-12}$ m/V. The attenuation of the macroscopic second-order NLO properties of the poled polymer films was theoretically analyzed in detail by considering the chromophore electrostatic interactions. The theoretical result of the relationship $\chi_{33}^{(2)}$ and $N$ agreed well with the experimental result measured by SHG signal intensity probing for the DCNP/PEK-c polymer system. We have demonstrated that the chromophore electrostatic interactions play a critical role in defining the maximum optical nonlinearity for a given polymer system.

**Acknowledgment.** We gratefully acknowledge the National Natural Science Foundation of China (The Foundation No.: 69990540), the Opening Project of Semiconductor Institute Region of State Key Laboratory on Integrated Optoelectronics (11E01), and the Foundation of Shandong University (Y34026 and Y34978).

## References and Notes

(1) Dalton, L. R. *Chem. Ind.* **1997**, *7*, 510.
(2) Krgal, H.; Hohmann, R.; Marheine, C.; Pott, W.; Pompe, G.; Neyer, A.; Diepold, T.; Obermeier, E. *Electron. Lett.* **1998**, *34*, 1396.
(3) Marder, S. R.; Kippelen, B.; Jen, A. K.-Y.; Peyghambarian, N. *Nature* **1997**, *388*, 845.
(4) Ahlheim, M.; Barzoukas, M.; Bedworth, P. V.; Desce, M. B.; Fort, A.; Hu, Z. Y.; Marder, S. R.; Perry, J. W.; Runser, C.; Staehelin, M.; Zysset, B. *Science* **1996**, *271*, 335.
(5) Marder, S. R.; Perry, J. W. *Science* **1994**, *263*, 1706.
(6) Jen, A. K.-Y.; Cai, Y.; Bedworth, P. V.; Marder, S. R. *Adv. Mater.* **1997**, *9*, 132.
(7) Wu, J. W.; Valley, J. F.; Ermer, S.; Binkley, E. S.; Kenney, J. T.; Lipscomb, G. F.; Lytel, R. *Appl. Phys. Lett.* **1991**, *58*, 225.
(8) Cai, Y. M.; Jen, A. K.-Y. *Appl. Phys. Lett.* **1995**, *67*, 299.
(9) Jiang, H.; Kakkar, A. K. *Adv. Mater.* **1998**, *10*, 1093.
(10) Kobagashi, J.; Matsura, T.; Sasaki, S.; Maruno, T. *Appl. Opt.* **1998**, *37*, 1032.
(11) Cook, J. P. D.; Este, G. O.; Shephered, F. R.; Westwood, W. D.; Arrington, J.; Moyer, W.; Nurse, J.; Powell, S. *Appl. Opt.* **1998**, *37*, 1220.
(12) Singer, K. D.; Kuzyk, M. G.; Sohn, J. E. *J. Opt. Soc. Am. B* **1987**, *4*, 968.
(13) Atkins, P. W. *Physics Chemistry*; W. H. Freeman and Company: New York, 1982; p 766.
(14) Dalton, L.; Harper, A.; Ren, A.; Wang, F.; Todorova, G.; Chen, J.; Zhang, C.; Lee, M. *Ind. Eng. Chem. Res.* **1999**, *38*, 8.
(15) Allen, S.; Mclean, T. D.; Gordon et, P. F.; Bothwell, B. D.; Hursthouse, M. B.; Karaulov, S. A. *J. Appl. Phys.* **1988**, *64*, 2583.
(16) Maker, P. D.; Terhune, R. W.; Nissenoff, M. *Phys. Rev. Lett.* **1962**, *8*, 21.
(17) Jerphagnon, J.; Kurtz, S. K. *J. Appl. Phys.* **1970**, *41*, 1667.
(18) Kuzyk, M. G.; Singer, K. D.; Zahn, H. E.; King, L. A. *J. Opt. Soc. Am. B* **1989**, *6*, 742.
(19) Herman, W. N.; Hayden, L. M. *J. Opt. Soc. Am. B* **1995**, *12*, 416.
(20) Singh, B. P.; Prasad, P. N. *J. Opt. Soc. Am. B* **1998**, *5*, 453.
(21) Pretre, P.; Wu, L.-M.; Knoesen, A.; Swalen, J. D. *J. Opt. Soc. Am. B* **1998**, *15*, 359.
(22) Sohn, J. E.; Singer, K. D.; Kuzyk, M. G. In Messier, J., Kajzar, F., Prasad, P., Ulrich, D., Eds.; *Orientationally Ordered Nonlinear Optical Polymer Films*; Kluwer Academic Publishers: Dordrecht, 1989; p 291.
(23) Bewsher, J. D.; Mitchell, G. R. *Appl. Opt.* **1997**, *36*, 7760.
(24) Coelho, R. *Physics of Dielectric for Engineer*; Elsevier Scientific Publishing Company: Paris, 1979; p 20.
(25) Kittol, C. *Introduction to Solid State Physics*; John Wiley & Sons: New York, 1976; p 100.
(26) Wu, J. W. *J. Opt. Soc. Am. B* **1991**, *8*, 142.
(27) Harper, A. W.; Sun, S.; Dalton, L. R.; Garner, S. M.; Chen, A.; Kalluri, S.; Steier, W. H.; Robinson, B. H. *J. Opt. Soc. Am. B* **1998**, *15*, 329.
(28) Hansen, J. P.; Mcdonald, I. R. *Theory of Simple Liquids*; Academic: London, 1976; p 395.

MA001737B